# Observation of J/$\psi p$ resonances consistent with pentaquark states in $\Lambda_b^0 \to \mathrm{J}/\psi K^- p$ decays

2018/11/05 이호빈

# Pentaquark

- Pentaquark is a particle which consists of four quarks and a antiquark.
- There were a few experiments results asserting discovery of pentaquarks.
- In 2015, LHCb has found the charmonium-pentaquark states.

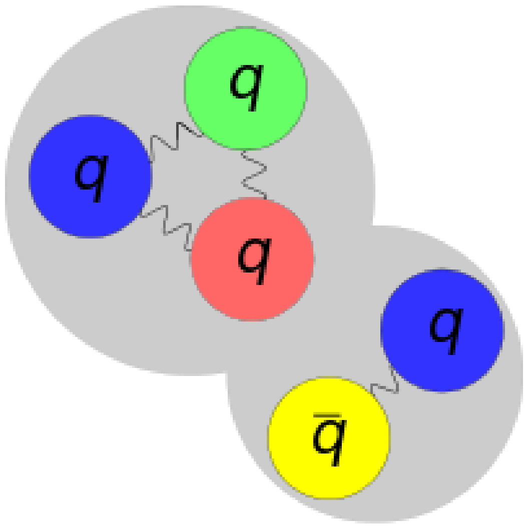


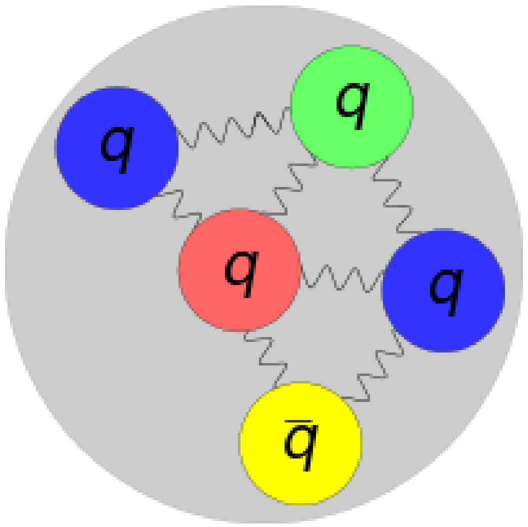


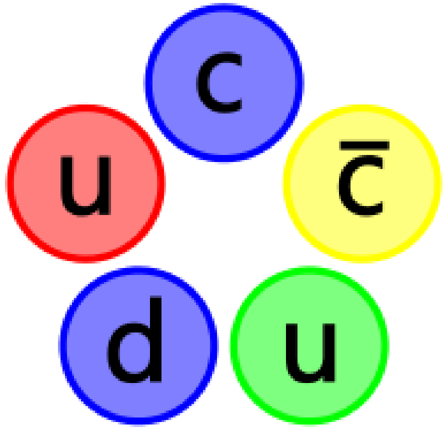

# Decay chain

$$\Lambda_b^0 \to J/\psi\ \Lambda^*$$
$$J/\psi \to J/\psi \to \mu^+\mu^-$$
$$\Lambda^* \to K^-\ p$$

$$\Lambda_b^0 \to P_c^+\ K^-$$
$$P_c^+ \to p\ J/\psi, \quad J/\psi \to \mu^+\mu^-$$
$$K^- \to K^-$$

Think of $\Lambda_b^0$-> $J/\psi K^- p$ decay

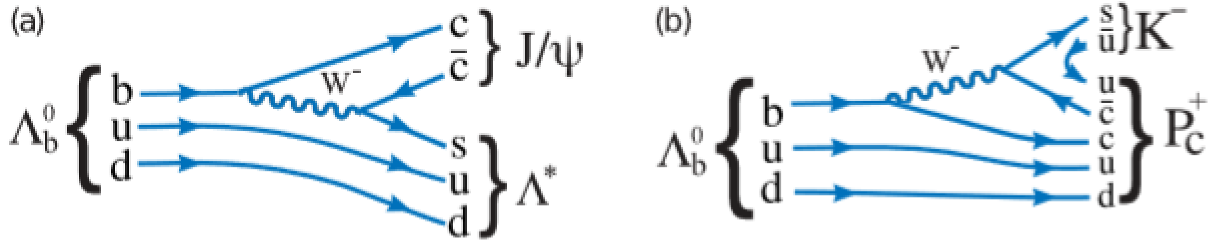

# Dalitz plot

- $m_{Kp}^2$= 2.3 GeV is corresponding to $\Lambda(1520)$ resonance
- There is a resonance $m_{Jp}^2$ = 19.5 GeV
- To see they are real resonance, full amplitude analysis based on helicity formalism is needed.

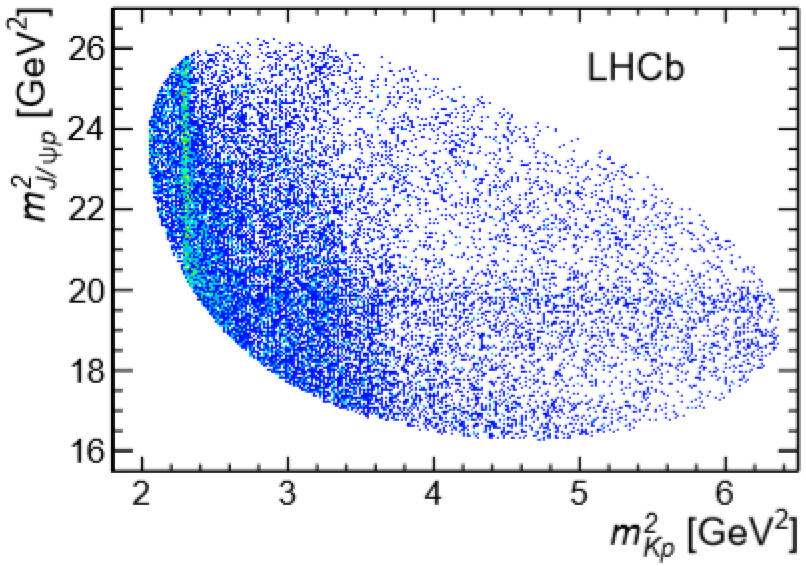


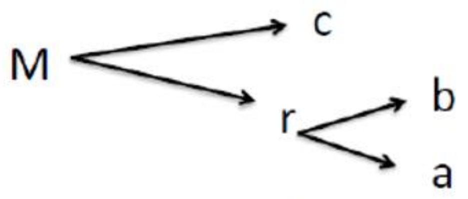


We can describe the behavior of the resonance by using a relativistic Breit-Wigner amplitude

$$\mathcal{A}_{BW} \sim \frac{1}{M_r^2 - s_{ab} - i\Gamma M_r} \; ; \quad \Gamma = \frac{\hbar}{\tau}$$

$\Gamma$ is inverse of lifetime $\tau$ of resonant state

# Environment of LHCb

- 7 TeV center of mass energy beam (1 $fb^{-1}$ of integrated luminosity)
- 8 TeV center of mass energy beam (2 $fb^{-1}$)

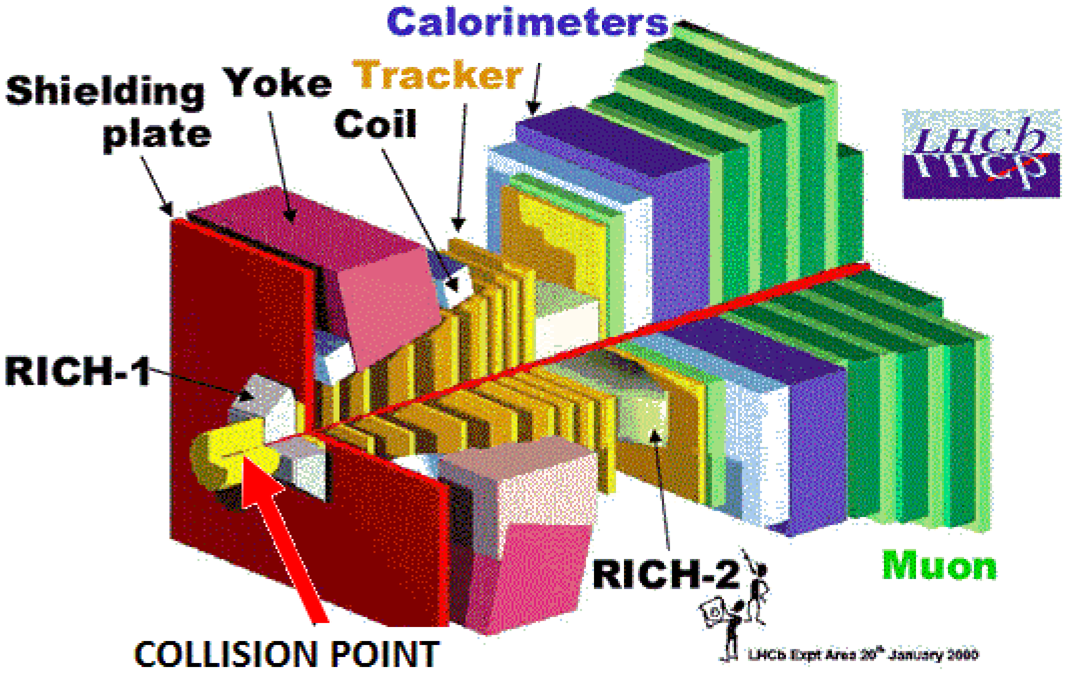

# Full amplitude analysis

A->BC Scattering amplitude =

$$\mathcal{H}^{A\to BC}_{\lambda_B,\lambda_C}\ D^{J_A}_{\lambda_A,\lambda_B-\lambda_C}(\phi_B,\theta_A,0)^* R_A(m_{BC}) = \mathcal{H}^{A\to BC}_{\lambda_B,\lambda_C}\ e^{i\lambda_A\phi_B}\ d^{J_A}_{\lambda_A,\lambda_B-\lambda_C}(\theta_A) R_A(m_{BC}),$$

$$\mathcal{H}^{A\to BC}_{\lambda_B,\lambda_C} = \sum_L \sum_S \sqrt{\frac{2L+1}{2J_A+1}} B_{L,S} \left(\begin{array}{cc|c} J_B & J_C & S \\ \lambda_B & -\lambda_C & \lambda_B-\lambda_C \end{array}\right) \times \left(\begin{array}{cc|c} L & S & J_A \\ 0 & \lambda_B-\lambda_C & \lambda_B-\lambda_C \end{array}\right), \quad (2)$$

$$J_A = L + S\,, \qquad S = J_B + J_C$$

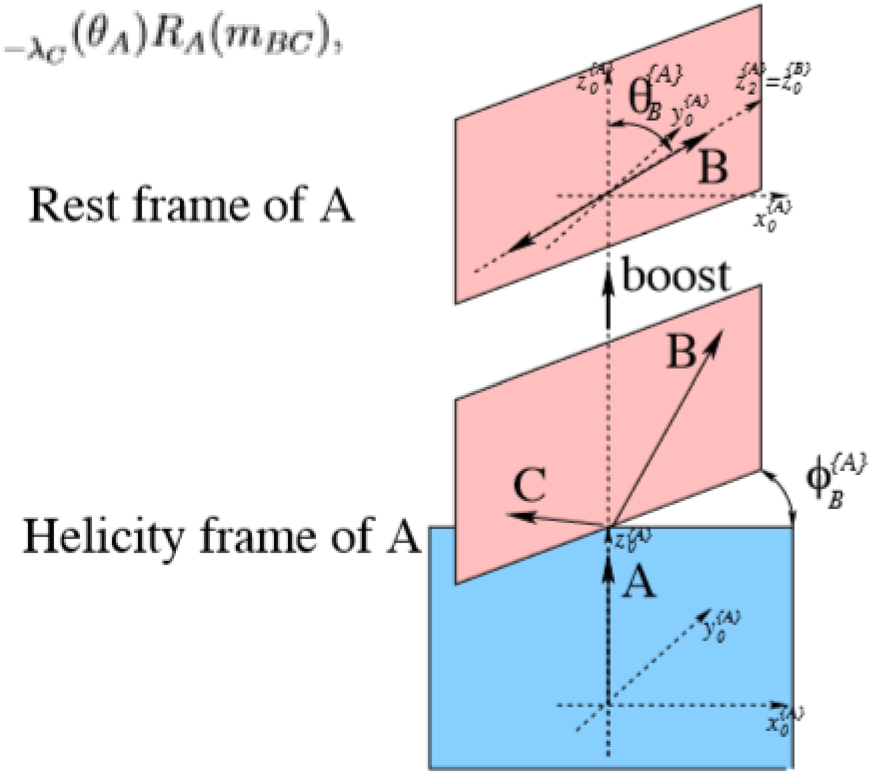


- H : decay helicity coupling (free parameter)
- D : wigner D-matrix
- R : additional factor

- Energy released from decay is small, higher L suppressed.

# Full amplitude analysis

$$\mathcal{M}^{\Lambda^*}_{\lambda_{\Lambda_b^0},\lambda_p,\Delta\lambda_\mu} \equiv \sum_n \sum_{\lambda_{\Lambda^*}} \sum_{\lambda_\psi} \mathcal{H}^{\Lambda_b^0\to\Lambda_n^*\psi}_{\lambda_{\Lambda^*},\lambda_\psi} D^{\frac{1}{2}}_{\lambda_{\Lambda_b^0},\lambda_{\Lambda^*}-\lambda_\psi}(0,\theta_{\Lambda_b^0},0)^*$$
$$\mathcal{H}^{\Lambda_n^*\to Kp}_{\lambda_p,0} D^{J_{\Lambda_n^*}}_{\lambda_{\Lambda^*},\lambda_p}(\phi_K,\theta_{\Lambda^*},0)^* R_{\Lambda_n^*}(m_{Kp})\, D^{1}_{\lambda_\psi,\Delta\lambda_\mu}(\phi_\mu,\theta_\psi,0)^*, \qquad (3)$$

- Independent parameter : $\theta_{\Lambda_b^0}, \theta_{\Lambda^*}, \theta_\psi, \phi_\mu, \phi_K, m_{Kp}$
- Possible coupling : 4 for $J_{\Lambda^*} = 1/2$, 6 for $J_{\Lambda^*} > 1/2$

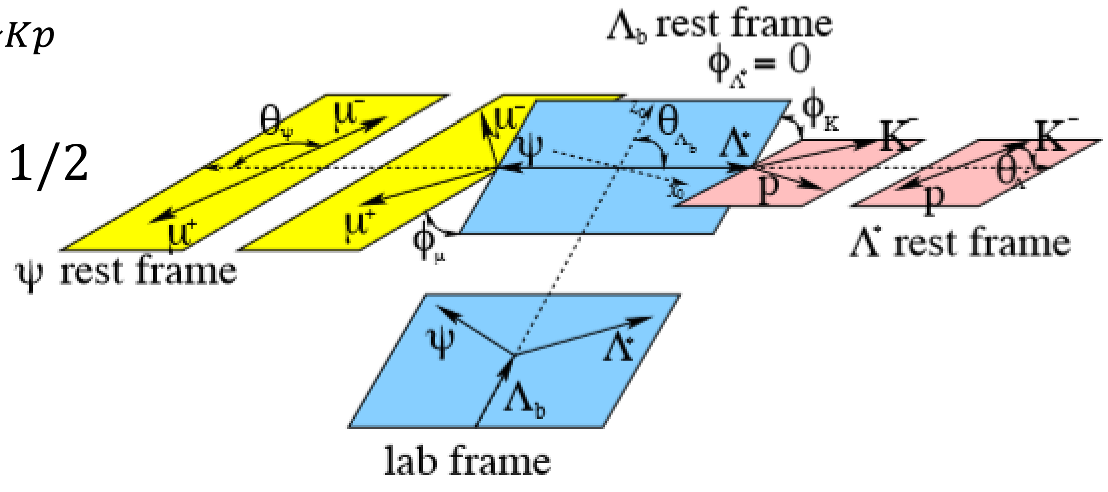

Figure 16: Definition of the decay angles in the $\Lambda^*$ decay chain.

# Full amplitude analysis

$$\mathcal{M}^{P_c}_{\lambda_{\Lambda_b^0},\lambda_p^{P_c},\Delta\lambda_\mu^{P_c}} \equiv \sum_j \sum_{\lambda_{P_c}} \sum_{\lambda_\psi^{P_c}} \mathcal{H}^{\Lambda_b^0\to P_{cj}K}_{\lambda_{P_c},0} D^{\frac{1}{2}}_{\lambda_{\Lambda_b^0},\lambda_{P_c}}(\phi_{P_c},\theta^{P_c}_{\Lambda_b^0},0)^*$$

$$\mathcal{H}^{P_{cj}\to\psi p}_{\lambda_\psi^{P_c},\lambda_p^{P_c}} D^{J_{P_{cj}}}_{\lambda_{P_c},\lambda_\psi^{P_c}-\lambda_p^{P_c}}(\phi_\psi,\theta_{P_c},0)^* R_{P_{cj}}(m_{\psi p})\;\; D^{1}_{\lambda_\psi^{P_c},\Delta\lambda_\mu^{P_c}}(\phi_\mu^{P_c},\theta_\psi^{P_c},0)^*, \quad (4)$$

The mass-dependent $R_{\Lambda_n^*}(m_{Kp})$ and $R_{P_{cj}}(m_{J/\psi p})$ terms are given by

$$R_X(m) = B'_{L^X_{\Lambda_b^0}}(p,p_0,d)\left(\frac{p}{M_{\Lambda_b^0}}\right)^{L^X_{\Lambda_b^0}} \mathrm{BW}(m|M_{0X},\Gamma_{0X})\, B'_{L_X}(q,q_0,d)\left(\frac{q}{M_{0X}}\right)^{L_X}. \quad (5)$$

$$\mathrm{BW}(m|M_{0X},\Gamma_{0X}) = \frac{1}{{M_{0X}}^2 - m^2 - iM_{0X}\Gamma(m)}, \quad (6)$$

where

$$\Gamma(m) = \Gamma_{0X}\left(\frac{q}{q_0}\right)^{2L_X+1}\frac{M_{0X}}{m}B'_{L_X}(q,q_0,d)^2, \quad (7)$$

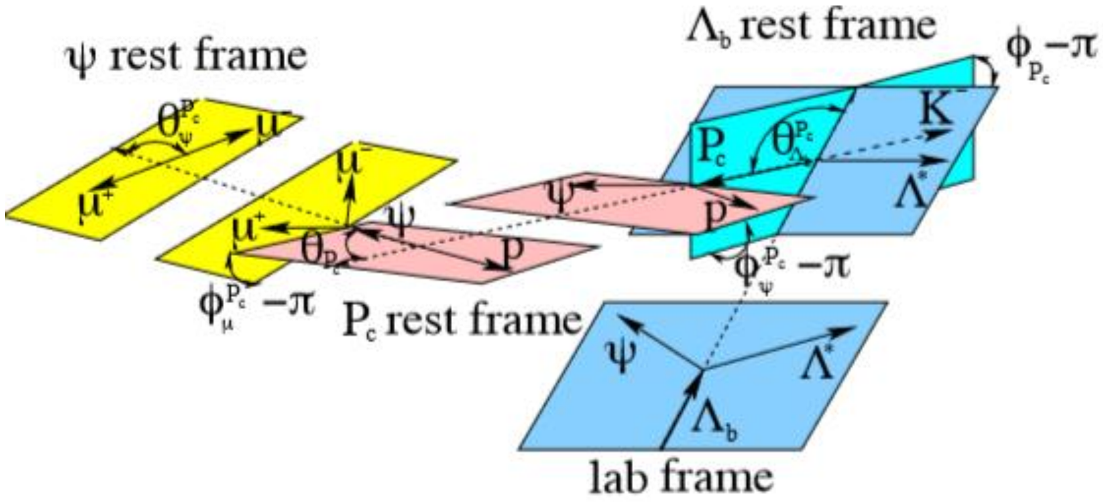


Figure 17: Definition of the decay angles in the $P_c^+$ decay chain.

- Possible coupling : 2 for $J_{P_c^+} = 1/2$, 3 for $J_{P_c^+} > 1/2$
- $p^L B_L$ → Blatt-Weisskopf functions

# Full amplitude analysis

- Muon and Proton are particles of the final state that should be observed.
- Relating the result of two decay chain is needed.
- Independent parameter : $\Omega = (\theta_{\Lambda_b^0}, \theta_{\Lambda^*}, \theta_{\psi}, \phi_{\mu}, \phi_K), m_{Kp}$

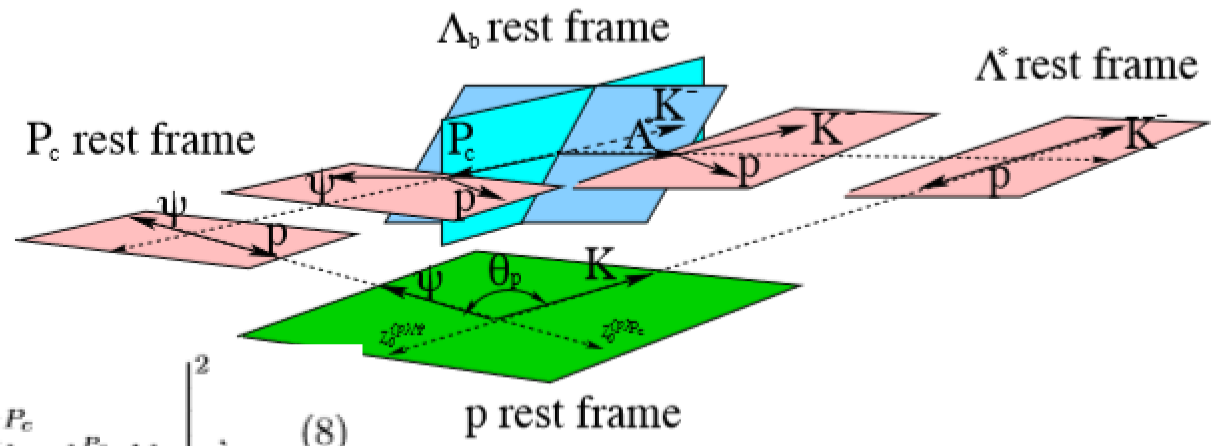


$$|\mathcal{M}|^2 = \sum_{\lambda_{\Lambda_b^0}} \sum_{\lambda_p} \sum_{\Delta\lambda_\mu} \left| \mathcal{M}^{\Lambda^*}_{\lambda_{\Lambda_b^0}, \lambda_p, \Delta\lambda_\mu} + e^{i\,\Delta\lambda_\mu \alpha_\mu} \sum_{\lambda_p^{P_c}} d^{\frac{1}{2}}_{\lambda_p^{P_c}, \lambda_p}(\theta_p)\, \mathcal{M}^{P_c}_{\lambda_{\Lambda_b^0}, \lambda_p^{P_c}, \Delta\lambda_\mu} \right|^2, \qquad (8)$$

Figure 18: Definition of the $\theta_p$ angle.

# Full amplitude analysis

- Use unbinned maximum likelihood fit
- Minimize $-2\ln\mathcal{L}(\overrightarrow{\omega}) = -2\ln\sum_i \mathcal{P}(m_{Kp\ i}, \Omega_i|\overrightarrow{\omega})$ respect to free parameter set $\vec{\omega}$

$$\mathcal{P}_{\text{sig}}(m_{Kp}, \Omega|\overrightarrow{\omega}) = \frac{1}{I(\overrightarrow{\omega})} \left|\mathcal{M}(m_{Kp}, \Omega|\overrightarrow{\omega})\right|^2 \Phi(m_{Kp})\epsilon(m_{Kp}, \Omega), \quad (69)$$

where $\Phi(m_{Kp})$ is the phase space function equal to $p\,q$, where $p$ is the momentum of the $Kp$ system (*i.e.* $\Lambda^*$) in the $\Lambda_b^0$ rest frame, and $q$ is the momentum of $K^-$ in the $\Lambda^*$ rest frame, and $I(\overrightarrow{\omega})$ is the normalization integral.

- Two independent fitting techniques with different background rejection schemes.

  -> Determine $\epsilon$ (selection efficiency)

# Full amplitude analysis

- With only Λ resonance

| State | $J^P$ | $M_0$ (MeV) | $\Gamma_0$ (MeV) | # Reduced | # Extended |
|---|---|---|---|---|---|
| $\Lambda(1405)$ | $1/2^-$ | $1405.1^{+1.3}_{-1.0}$ | $50.5 \pm 2.0$ | 3 | 4 |
| $\Lambda(1520)$ | $3/2^-$ | $1519.5 \pm 1.0$ | $15.6 \pm 1.0$ | 5 | 6 |
| $\Lambda(1600)$ | $1/2^+$ | 1600 | 150 | 3 | 4 |
| $\Lambda(1670)$ | $1/2^-$ | 1670 | 35 | 3 | 4 |
| $\Lambda(1690)$ | $3/2^-$ | 1690 | 60 | 5 | 6 |
| $\Lambda(1800)$ | $1/2^-$ | 1800 | 300 | 4 | 4 |
| $\Lambda(1810)$ | $1/2^+$ | 1810 | 150 | 3 | 4 |
| $\Lambda(1820)$ | $5/2^+$ | 1820 | 80 | 1 | 6 |
| $\Lambda(1830)$ | $5/2^-$ | 1830 | 95 | 1 | 6 |
| $\Lambda(1890)$ | $3/2^+$ | 1890 | 100 | 3 | 6 |
| $\Lambda(2100)$ | $7/2^-$ | 2100 | 200 | 1 | 6 |
| $\Lambda(2110)$ | $5/2^+$ | 2110 | 200 | 1 | 6 |
| $\Lambda(2350)$ | $9/2^+$ | 2350 | 150 | 0 | 6 |
| $\Lambda(2585)$ | ? | ≈2585 | 200 | 0 | 6 |

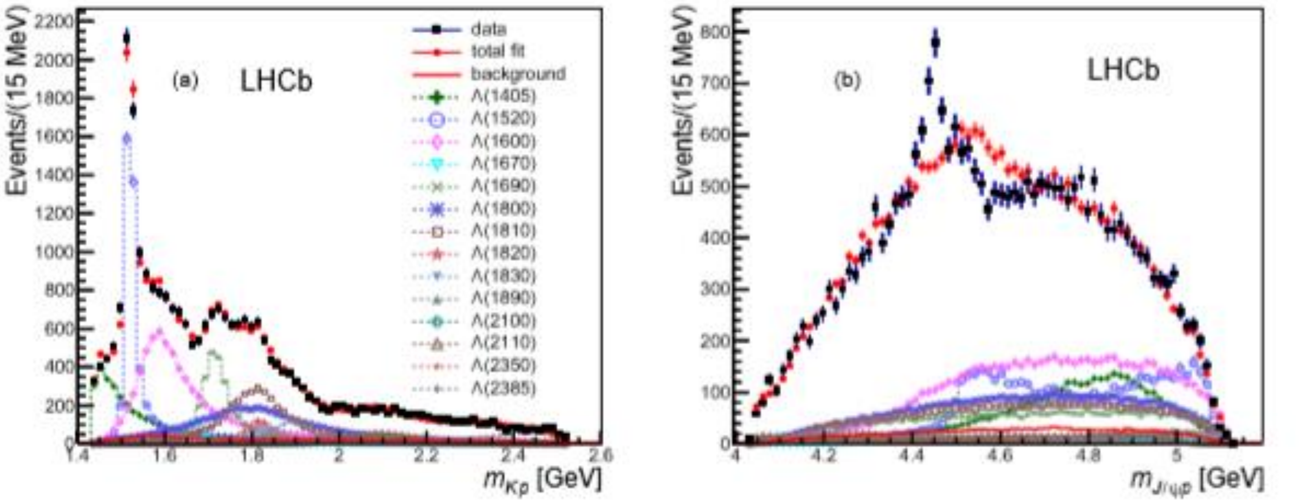


Figure 6: Results for (a) $m_{Kp}$ and (b) $m_{J/\psi p}$ for the extended $\Lambda^*$ model fit without $P_c^+$ states. The data are shown as (black) squares with error bars, while the (red) circles show the results of the fit. The error bars on the points showing the fit results are due to simulation statistics.

# Full amplitude analysis

- With $P_c^+(4380)$ with $J^p = 3/2^+$ , $P_c^+(4450)\ with\ J^p = 5/2^-$
- From null hypothesis, confidence levels are $9\sigma$ and $12\sigma$, respectively.
- Low M = 4380$\pm$ 8 $\pm$ 28 MeV and a width of 205 $\pm$ 18 $\pm$ 86 MeV
- High M = 4449.8$\pm$ 1.7 $\pm$ 2.5 MeV and a width of 39 $\pm$ 5 $\pm$ 19 MeV

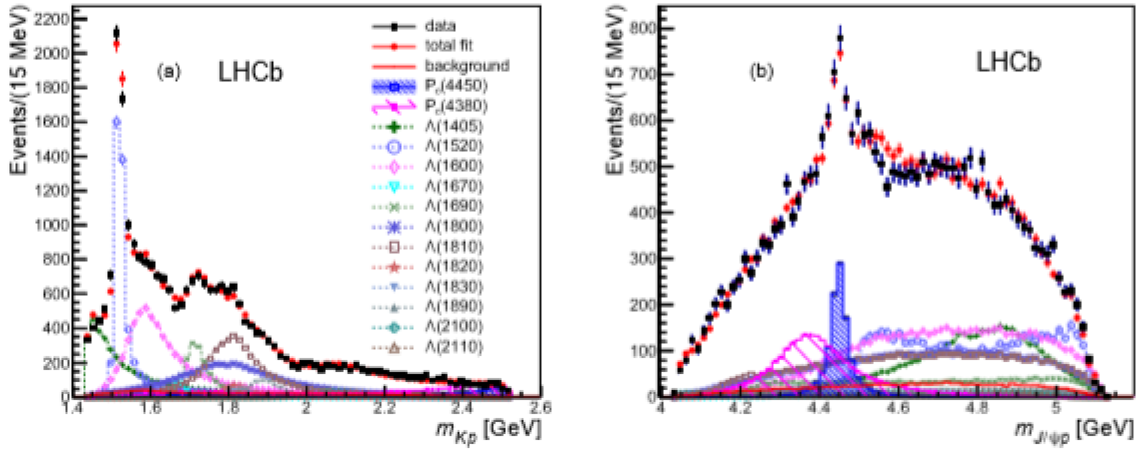


Figure 3: Fit projections for (a) $m_{Kp}$ and (b) $m_{J/\psi p}$ for the reduced $\Lambda^*$ model with two $P_c^+$ states (see Table 1). The data are shown as solid (black) squares, while the solid (red) points show the results of the fit. The solid (red) histogram shows the background distribution. The (blue) open squares with the shaded histogram represent the $P_c(4450)^+$ state, and the shaded histogram topped with (purple) filled squares represents the $P_c(4380)^+$ state. Each $\Lambda^*$ component is also shown. The error bars on the points showing the fit results are due to simulation statistics.

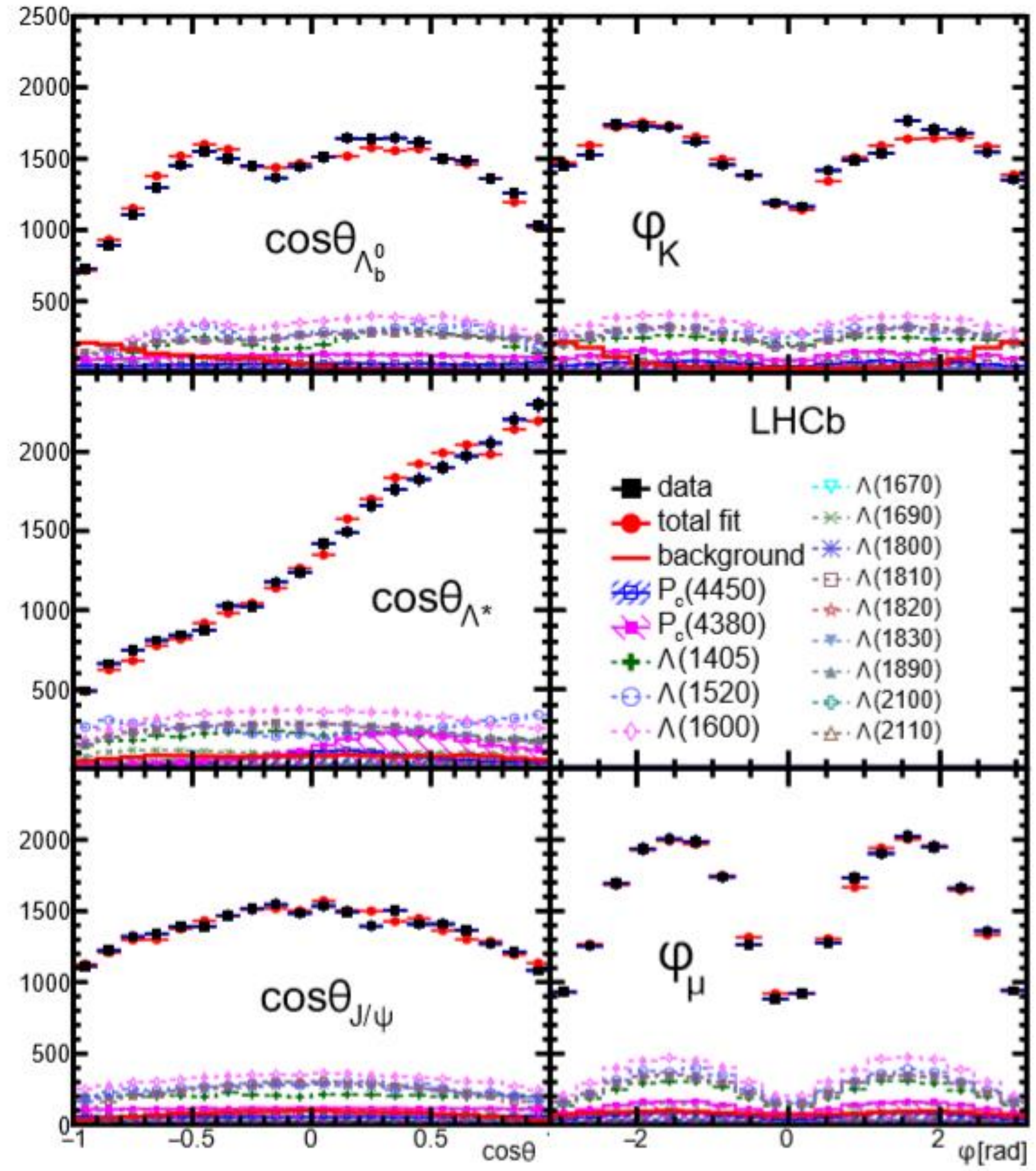


Figure 7: Various decay angular distributions for the fit with two $P_c^+$ states. The data are shown as (black) squares, while the (red) circles show the results of the fit. Each fit component is also shown. The angles are defined in the text.